

5-Axis Freeform Surface Milling using Piecewise Ruled Surface Approximation *

Gershon Elber

Department of Computer Science
Technion, Israel Institute of Technology
Haifa 32000, Israel

Russ Fish

Department of Computer Science
University of Utah
Salt Lake City, UT 84112 USA

March 14, 1994

Abstract

This paper presents a 5-axis side milling scheme for freeform surfaces based on automatic piecewise ruled surface approximation.

With this scheme, resulting surface finish is accurate and pleasing, and with a smaller scallop height compared to ball-end milling. The ruled surface approximation can be made arbitrarily precise resulting in an overall fast milling operation that satisfies tight tolerances, and nice surface finish.

The class of surfaces that can take advantage of this type of 5-axis milling operation includes both convex and saddle-like (hyperbolic) shapes.

1 Introduction

The automatic toolpath generation for manufacturing of models consisting of freeform surfaces is a difficult problem that has been addressed by numerous researchers [1, 4, 5, 6, 12, 13, 17, 18, 19, 20, 21, 22].

3-axis machining [1, 4, 17, 18, 19, 20, 21, 22], is more frequently used than 4- or 5-axis machining modes. While deriving a multi (i.e. 4- or 5-) axis toolpath is a relatively simple task, resolving the *tool accessibility* question can be difficult. Finding out whether the tool can access the surface without gouging into it, is significantly more difficult when

*This work was supported in part by DARPA (N00014-91-J-4123). All opinions, findings, conclusions or recommendations expressed in this document are those of the authors and do not necessarily reflect the views of the sponsoring agencies.

a tool can be arbitrarily oriented. We differentiate between *local accessibility* and *global accessibility*. The former can be resolved by inspecting only the neighborhood of the tip of the tool. The latter must take into consideration all other surfaces, or objects that can interfere with the tool or its holder. Clearly, resolving the local tool accessibility is easier. In this paper, we do not strive to solve the global tool accessibility problem, and only show how the presented milling approach can guarantee local access.

The larger the machining tool, the smaller the resulting scallop height. Moreover, larger tools reduce machining times. A nice finish usually result using flat end tools (see Plates 1 and 2). Further, machining using ball-end tools is slow because of a vanishing cutting speed at the tip of the tool, an impediment that shows up in neither the 5-axis flat end milling mode nor in the 5-axis side milling approach proposed herein.

Limited research has been conducted toward the use of 4- and 5-axis freeform surface machining. In [6], an attempt was made using local surface analysis to compute 5-axis flat-end toolpaths for freeform surfaces that are generally convex but with local and isolated non-convex regions. No discussion is made how the convex regions can be detected and isolated. Furthermore, only local accessibility is considered and resolved numerically. In [16], a robust optimization method is derived, based on global symbolic shape analysis, to automatically detect and differentiate the surface regions that can be machined using a flat end tool in a 5-axis mode and the surface regions that must be machined using a ball end tool in a 3- or 5-axis mode. In [12], a scheme for the generation of almost optimal toolpath for freeform surfaces is derived, based on iso-parametric curves. By utilizing iso-parametric curves, the resulting toolpath is exact and compact as opposed to contoured piecewise linear data. By extracting iso-parametric curves adaptively, the length of the toolpath is optimized. Moreover, this scheme of adaptive iso-parametric curves can also be employed for 5-axis flat-end milling, as is done for example in [13].

Tool accessibility, in 5-axis machining modes, is a most difficult and challenging problem. In [3], an attempt is made to classify the directions from which a model is accessible by deriving the Gauss map [7], \mathcal{G} and the visibility map, \mathcal{V} , of the model. While \mathcal{G} is well known from the field of differential geometry [7], \mathcal{V} introduces the set of all directions from which a surface is completely visible. In [14], we extend this notion to freeform surfaces. This classification solves only local accessibility and does not detect global interference. In [13], a method is suggested that provides a solution for the global interference problem for machined surfaces that are convex. This method reduces the 5-axis global accessibility problem into a 3-axis global accessibility problem that is easier to resolve, by warping the space above the machined surface. The method in [13], can always be utilized whenever an operation of 5-axis flat-end mill that is normal to the surface is feasible.

In this paper, we propose an approach to 5-axis machining that would extend the class of machinable freeform surfaces to include both convex and saddle-like (hyperbolic) surfaces. This paper is organized as follows. Section 2 describes how a ruled surface approximation can be derived to an arbitrary piecewise polynomial or rational surface using the B-spline tensor product representation, following [15]. In section 3, we exploit this surface approximation to formulate a side milling technique for convex and saddle-like surfaces. Section 4 presents some results on several convex and saddle-like surfaces while conclusions and future work are discussed in section 5.

All presented results, including the machined parts, were created with the aid of Alpha_1, a NURBs based solid modeling system that is being developed at the University of Utah.

2 Piecewise Ruled Surface Approximation

Let $S_1(u, v)$ and $S_2(r, s)$ be two parametric surfaces.

Definition 1 *The distance between point $S_1(u_0, v_0)$ and surface $S_2(r, s)$ is*

$$Dist(S_1(u_0, v_0), S_2(r, s)) = \min_{r, s} \|S_1(u_0, v_0) - S_2(r, s)\|. \quad (1)$$

Definition 2 *The distance between two surfaces $S_1(u, v)$ and $S_2(r, s)$ is*

$$Dist(S_1(u, v), S_2(r, s)) = \max_{u, v} \min_{r, s} \|S_1(u, v) - S_2(r, s)\|. \quad (2)$$

Let $S(u, v)$ be a polynomial B-spline surface. Let $C_1(u) = S(u, Vmin)$ and $C_2(u) = S(u, Vmax)$ be the $Vmin$ and $Vmax$ boundary curves of $S(u, v)$ respectively. Assume $C_1(u) \neq C_2(u)$. Let,

$$R(u, v) = vC_1(u) + (1 - v)C_2(u), \quad 0 \leq v \leq 1, \quad (3)$$

be the ruled surface constructed between $C_1(u)$ and $C_2(u)$. Let $\hat{R}(u, v)$ be the representation for $R(u, v)$ in the same function space as $S(u, v)$. That is, \hat{R} and S share the same v order and continuity (knot vector). $\hat{R}(u, v)$ can be obtained from $R(u, v)$ via appropriate degree raising [8, 9] and refinement [2, 10] of the linear (ruled) direction, v . Then,

$$\max_{u, v} \|S(u, v) - \hat{R}(u, v)\|$$

$$\begin{aligned}
&= \max_{u,v} \left\| \sum_{i=0}^m \sum_{j=0}^n P_{ij} B_{i,\tau}^m(u) B_{j,\xi}^n(v) - \sum_{i=0}^m \sum_{j=0}^n Q_{ij} B_{i,\tau}^m(u) B_{j,\xi}^n(v) \right\| \\
&= \max_{u,v} \left\| \sum_{i=0}^m \sum_{j=0}^n (P_{ij} - Q_{ij}) B_{i,\tau}^m(u) B_{j,\xi}^n(v) \right\| \\
&\leq \max(\|P_{ij} - Q_{ij}\|, \forall i, j),
\end{aligned} \tag{4}$$

since the B-spline basis functions are nonnegative and sum to one. Equation (4) provides a simple mechanism to bound the maximum distance between surface S and the ruled surface R (\hat{R}) since,

$$\begin{aligned}
Dist(S(u, v), \hat{R}(r, s)) &= \max_{u,v} \min_{r,s} \|S(u, v) - \hat{R}(r, s)\| \\
&\leq \max_{u,v} \|S(u, v) - \hat{R}(u, v)\| \\
&\leq \max(\|P_{ij} - Q_{ij}\|, \forall i, j).
\end{aligned} \tag{5}$$

An algorithm to approximate an arbitrary tensor product surface as a set of ruled surfaces is derived in Algorithm 1 based on this process. In Algorithm 1 and based on equation (5), the function **maxDistance** returns an upper bound on the distance between the original surface S and its ruled surface approximation. In [15], we discuss the quality of the bound, the generalization of the distance computation (equation (4)) for rational surfaces, and possible approaches for improvements on the distance bound in non uniform parametrization.

Algorithm 1 returns a set of ruled surfaces that approximates the original surface S to within the required tolerance τ . Figure 1 shows an example of four consecutive stages of Algorithm 1.

3 The Toolpath Generation algorithm

A ruled surface can be side milled with high precision, by approximating an offset [11] of tool radius to the ruled surface. The axis of the tool is then aligned with the ruled parametric direction v , $C_1(u) - C_2(u)$ (equation (3)), of the offset of the ruled surface. With the aid of Algorithm 1, one can approximate an arbitrary surface with a set of ruled surfaces. With the aid of equation (5), the error of the approximation can be globally bounded. The toolpath for each offset approximation of each ruled surface is then generated so that the side of the mill is tangent to the ruled surface, in the ruled parametric direction v .

Algorithm 1 can be used to generate a piecewise ruled surface approximation for a concave surface. Unfortunately, the side milling tool will gouge into the surface at

Algorithm 1

Input:

$S(u, v)$, surface to be approximated using ruled srfs in v .
 τ , tolerance of piecewise ruled approximation to be used.

Output:

\mathcal{R} , Set of ruled surfaces, approximating $S(u, v)$ to within τ .

Algorithm:

```

RuledSrfApproximation(  $S$ ,  $\tau$  )
begin
   $C_1(t), C_2(t) \Leftarrow Vmin$  and  $Vmax$  boundary of  $S$ ;
   $R \Leftarrow$  ruled surface between  $C_1(t)$  and  $C_2(t)$ ;
   $\hat{R} \Leftarrow R$  refined and degree raised in  $v$  to match  $S$ ;
  If (  $\maxDistance( S, \hat{R} ) < \tau$  )
    return {  $R$  };
  else
    begin
      Subdivide  $S$  into two subsrfs  $S^1, S^2$  along  $v$ ;
      return
        RuledSrfApproximation(  $S^1, \tau$  )  $\cup$ 
        RuledSrfApproximation(  $S^2, \tau$  );
    end
  end
end

```

every location. However, and unlike 5-axis flat-end milling operation, the piecewise ruled surface approximation can be employed to generate locally gouge free toolpaths for machining hyperbolic or parabolic surface regions. Exploiting differential geometry, exactly one of the two principal curvatures is negative (zero), at an hyperbolic (parabolic) point [7]. For convex-elliptic, hyperbolic, and parabolic regions, there always exist a locally gouge free direction, in the tangent plane of the surface, that can be used to orient the axis of the tool (see Figure 2). That direction is a principal direction that is associated with a negative (zero for a parabolic point) normal curvature. The piecewise ruled surface approximation should be computed so that the ruled direction has a positive normal curvature in no location on the surface, for a locally gouge free toolpath.

An algorithm to generate a side milling toolpath can now be derived and is shown in Algorithm 2. The surface offset approximation stage and the piecewise ruled surface

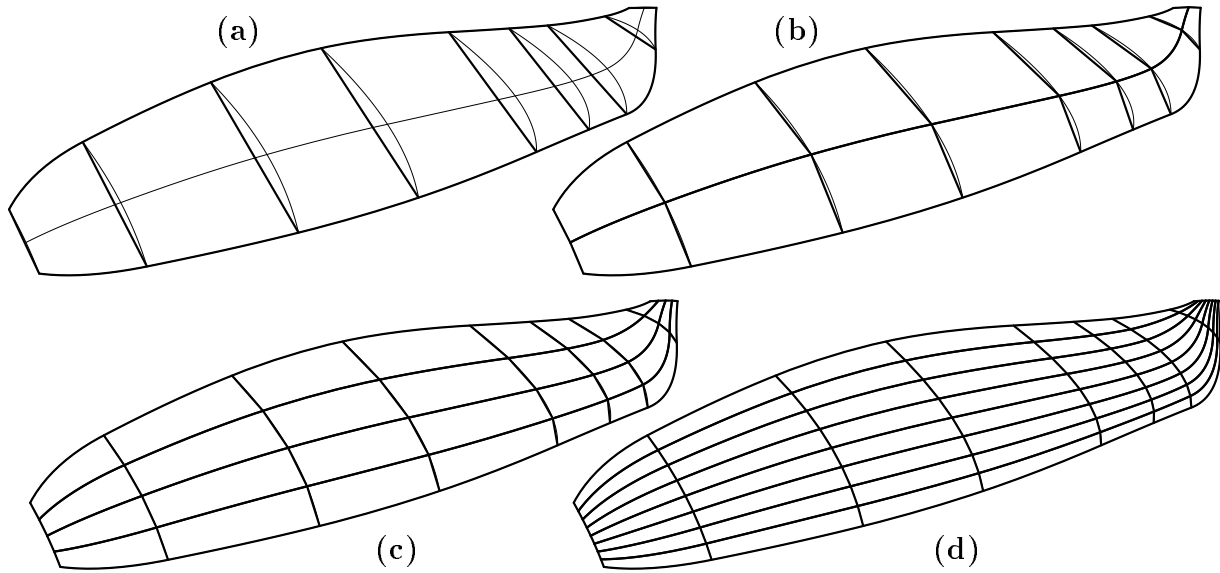


Figure 1: Four stages in approximating a surface with piecewise ruled surfaces (Alg. 1).

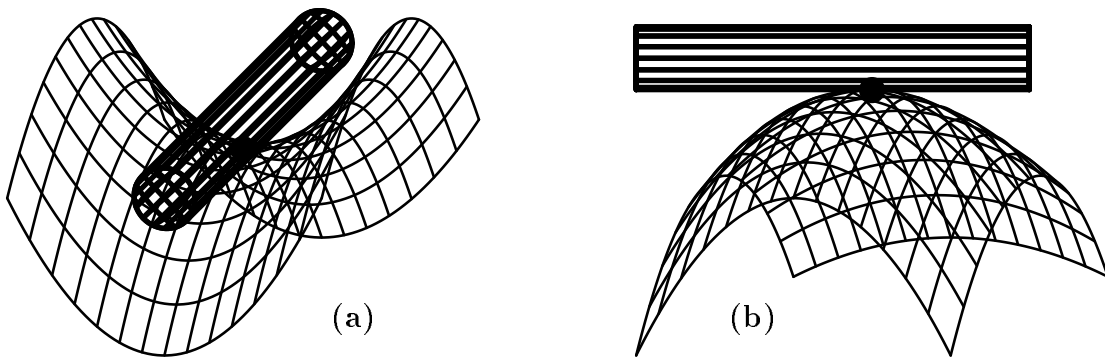


Figure 2: A saddle-like surface can be side milled (a) from a set of directions in the tangent plane of the surface, without *locally gouging* into the surface, while a convex surface can be side milled (b) from any direction in the tangent plane of the surface, without *locally gouging* into the surface.

approximation stage (stages (1) and (2) in Algorithm 2), may be interchanged. One can consider computing the offset to the input surface S and then apply the piecewise ruled surface approximation to the offset surface. Alternatively, the piecewise ruled surface approximation can be applied directly to S and then offset surfaces of ruled surfaces are computed as a second stage. In our implementation, discussed in section 4, the offset was first computed on S .

Algorithm 2

Input:

- $S(u, v)$, surface to be machined.
- τ , tolerance of piecewise ruled approximation in v direction.
- r , tool radius for the side milling.

Output:

- \mathcal{T} , Set of toolpath curves to machine $S(u, v)$ to within τ .

Algorithm:

- ```

RuledToolPath(S , τ)
begin
(1) $\mathcal{S}_r \Leftarrow S$ offset by r ;
(2) $\mathcal{R} \Leftarrow$ RuledSrfApproximation(\mathcal{S}_r , τ) in v direction;
 $\mathcal{T} \Leftarrow$ toolpath derived directly from \mathcal{R} ;
end

```

## 4 Examples

A simple example of a toolpath created using Algorithm 2 can be seen in Figure 3. Shown are the original surface, which is a part of a turbine blade, and the toolpath created from the ruled surface approximation.

A computer model of a propeller of a model airplane was also used as a test case. The model is shown in Figure 4. Figure 5 shows the toolpath generated for the top section of the propeller's blade. The bottom section was machined in a similar way. This surface has both convex and saddle-like regions and the toolpath was generated so that the tool axis is roughly perpendicular to the major axis of the blade, preventing gouging. Plate 1 shows two machined propellers from aluminum with (top) and without (middle) their fixture along with an original wooden propeller (bottom).

A more complex example is shown in Figure 6. This blade of a marine propeller was similarly processed and approximated using a set of ruled surfaces. Figure 7 shows the piecewise ruled surface approximation for the top side of the blade while Figure 8 shows the derived toolpath. In Plate 2, the final part with the top side machined from aluminum is shown.

A relatively large tool can be usually used in this type of machining. For the propeller of the model airplane, a 0.75" (diameter) tool was used while for the blade of the

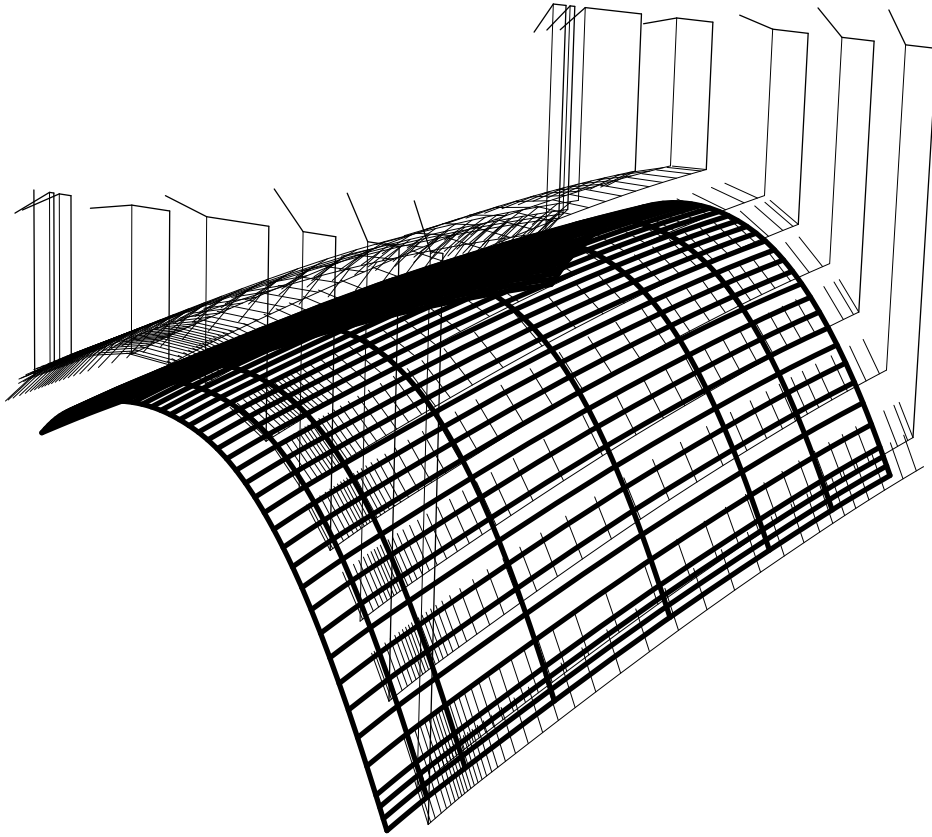


Figure 3: A simple example of the piecewise ruled surface side milling approach. The computed 5-axis side milling toolpath is shown with small vectors along the toolpath indicating the orientation of the tool. In this toolpath, the tool is retracted after each ruled surface path.

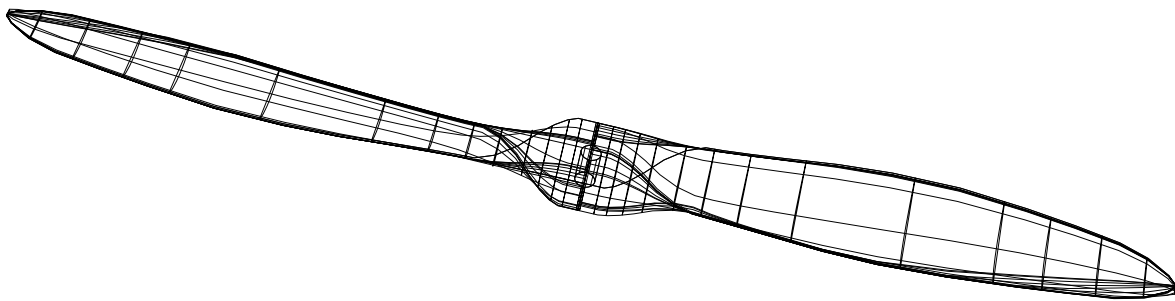


Figure 4: A propeller of a model airplane has blades with only convex and saddle-like regions which can be machined using the piecewise ruled surface side milling technique.



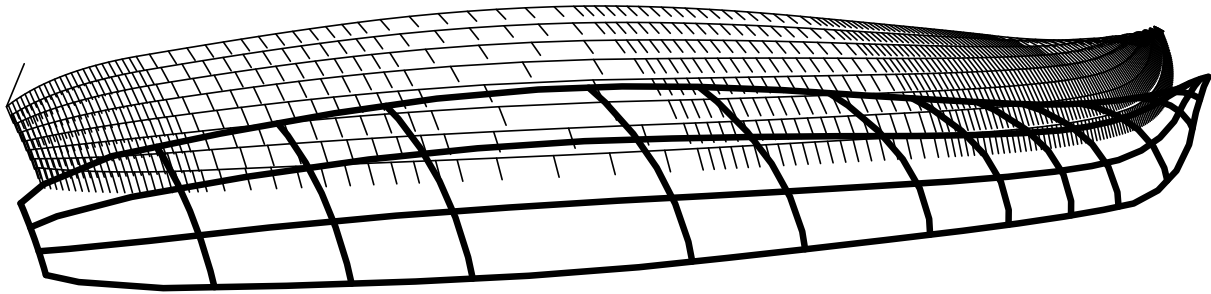


Figure 5: The toolpath for the top surface of the blade of the propeller in Figure 4. See Plate 1 for a picture of the machined propeller. Shown is a zigzag toolpath for which the tool is retracted after all ruled surface paths are being executed.

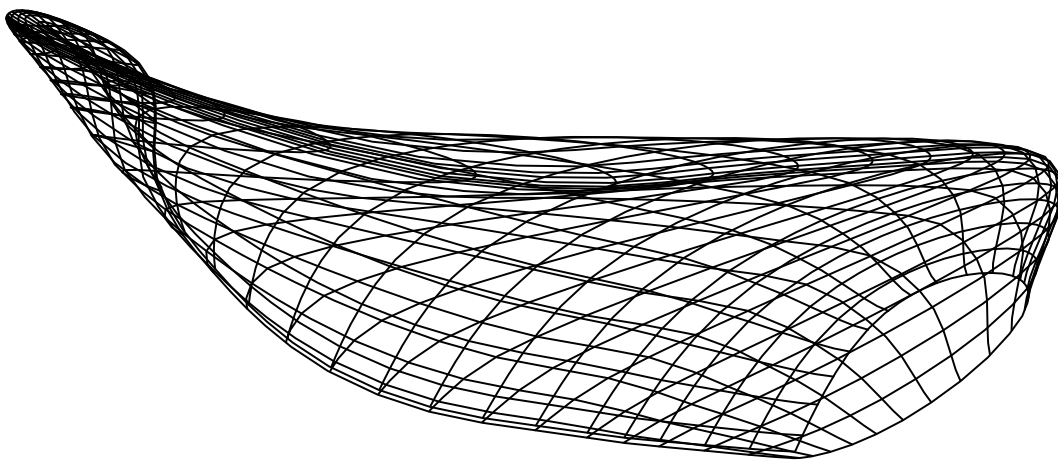


Figure 6: A blade of a marine propeller.

marine propeller, a 1" tool was selected. As a result, the machining operations can be accelerated. Machining of the top part of the blade of the marine propeller took several minutes while manufacturing the entire propeller of the model airplane, with four fixtures, has been accomplished in far less than an hour.

Algorithm 2, when applied to a surface that is ruled, generates a single pass toolpath as one would expect. The air flow tunnels for the centrifugal compressor in Plate 3 were machined using a tapered tool, shaped as a rounded-end truncated cone. The computation of the offset of the piecewise ruled surfaces must compensate for the angle of the tool axis and the line of tangency between the tool and the machined surface. Figure 9 shows the toolpath that was generated and the geometry of the wall of the tunnel, for two different blades.

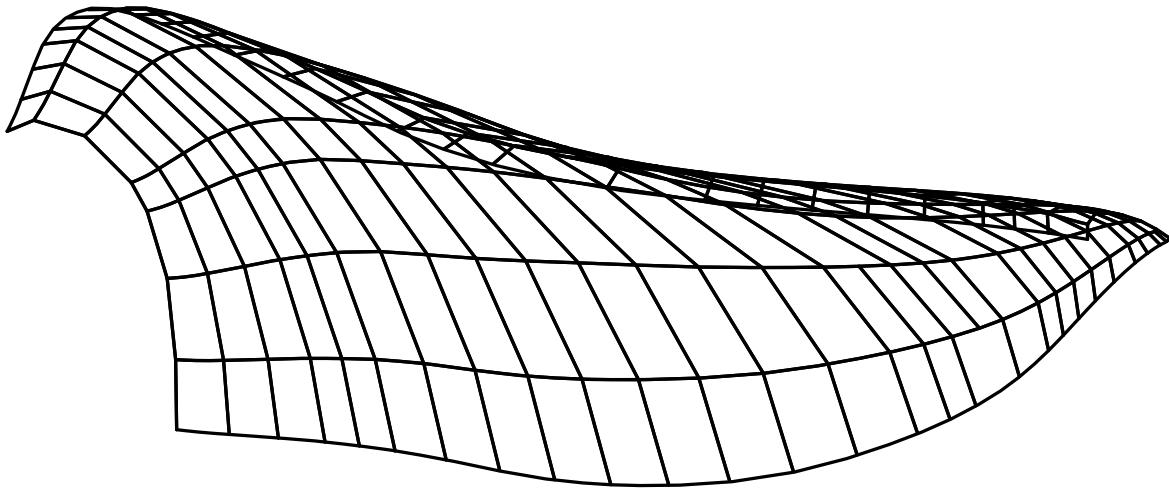


Figure 7: Piecewise ruled surface approximation of the top portion of the marine propeller from Figure 6. The approximation herein is about half as fine as is used to machine the aluminum part in Plate 2.

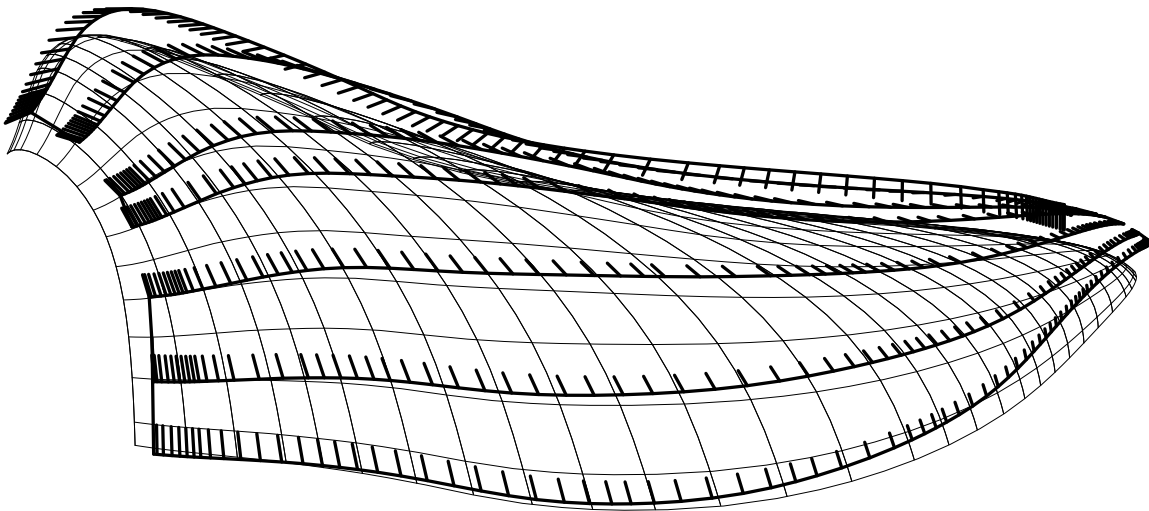


Figure 8: The toolpath for the top side of the blade of this marine propeller was generated using the piecewise ruled surface approximation technique (Figure 7). See Plate 2 for a picture of the machined part.

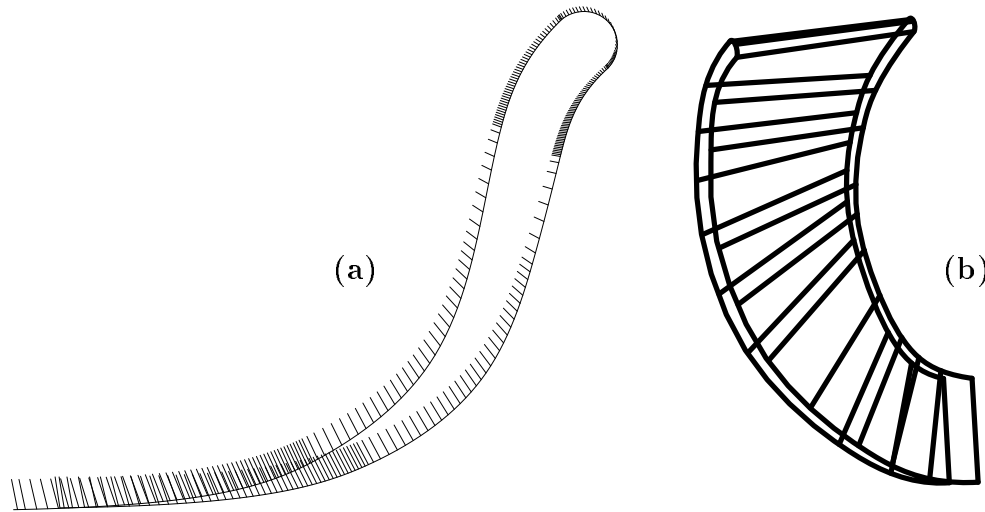


Figure 9: The toolpath for the side walls of the centrifugal compressor. The geometry (a) and the toolpath (b) are shown for different blades. In this case, the tool used was not cylindrical but tapered, shaped as a rounded-end truncated cone. See Plate 3 for a picture of the machined part.

## 5 Conclusion and Future Work.

This paper presents a method for machining saddle-like (hyperbolic) and convex surfaces using 5-axis side milling. This method extends the class of surfaces that can be machined in 5-axis mode from convex surfaces using flat-end tools, to convex and saddle-like surfaces using side milling.

In the examples of section 4, an iso-parametric direction for which the normal curvature is always negative was manually selected to align the tool axis. One can always evaluate the directions, in the tangent plane of the surface, of the principal curvatures and exploit them to compute the piecewise ruled surface approximation direction. The ruled direction can be set to be the direction in the tangent plane of the surface closest to a minimal negative principal curvature for the saddle-like case. Further, the maximal principal curvature can be employed to directly bound the largest tool radius that can be used for the machining operation of saddle-like regions.

The toolpath generated using the piecewise ruled surface approximation consists of iso-parametric curves only. It is perceivable that the toolpath can be optimized using similar technique to those used to generate the adaptive iso-parametric curve toolpath in [12]. This direction should be further investigated.

Extending this algorithm to support trimmed surfaces is simple and can be accomplished by trimming the ruled surface approximation appropriately. Figure 10 shows a simple example of a trimmed saddle surface with its piecewise ruled surface approxima-

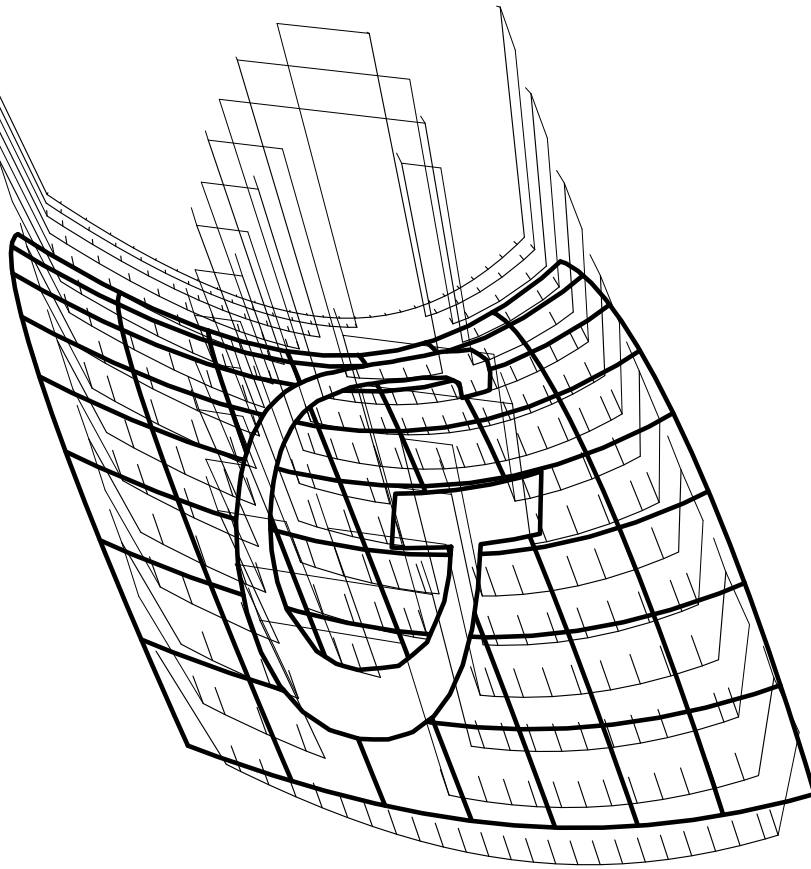


Figure 10: Piecewise ruled surface approximation of a trimmed saddle surface, from which a letter G was subtracted, is used to generate 5-axis side milling toolpath.

tion driven toolpath.

This paper does not address global accessibility issues for 5-axis machining operations. Several methods are known for the simulation, verification, and generation of 3-axis machining toolpaths for freeform surfaces. Most noticeably, Z-buffer and Z-depth techniques [20, 21] are becoming popular even in low end machines. Unfortunately, this problem is yet to be solved for 5-axis milling operations, so that 5-axis milling operations can be exploited to their full potential. Toward that end we define the following.

**Definition 3** *A surface region,  $S$ , is considered ball-end accessible with respect to ball-end tool of radius  $r$ , if any point on  $S$  can be tangent to a ball-end tool of radius  $r$  so that the tool does not gouge to any other part of the model containing  $S$ .*

The computation of the accessibility of ball-end cutters is recognized as an important problem since it is used in traditional 3-axis and 5-axis ball-end machining. However,

the side milling approach presented in this paper requires the derivation of a different accessibility consideration,

**Definition 4** *A surface region,  $S$ , is considered cylindrically accessible with respect to a given cylinder of radius  $r$ , if any point on  $S$  can be tangent to the side of the cylinder so that the cylinder does not gouge to any other part of the model containing  $S$ .*

The computation of the accessibility of tools in 5-axis milling operations remains an intriguing and challenging problem. The solution to this problem will pave the way to the general use of 5-axis milling operations.

## 6 Acknowledgment

The authors are grateful to Samuel Drake for helping in testing these algorithms and for the model of the centrifugal compressor and to Elaine Cohen for her valuable remarks on the various drafts of this paper.

## References

- [1] J. E. Bobrow. NC Machine Tool Path Generation From CSG Part Representations. *Computer Aided Design*, vol. 17, no. 2, pp 69-76, March 1985.
- [2] W. Boehm. Inserting New Knots into B-spline Curves. *Computer Aided Design*, vol. 12, no. 4, pp 199-201, July 1980.
- [3] L. L. Chen, S. Y. Chou, and T. C. Woo. Separating and Intersecting Spherical Polygons: Computing Machinability of Three-, Four- and Five-Axis Numerically Controlled Machines. *Transaction on Graphics*, Vol. 12, No. 4, pp 305-326, October 1993.
- [4] B. K. Choi and C. S. Jun. Ball-End Cutter Interference Avoidance in NC Machining of Sculptured Surfaces. *Computer Aided Design*, vol. 21, no. 6, pp 371-378, July/August 1989.
- [5] B. K. Choi, J. W. Park, and C. S. Jun. Cutter-location data optimization in 5-axis surface machining. *Computer Aided Design*, vol. 25, no. 6, pp 377-386, June 1993.
- [6] J. J. Chou. Numerical Control Milling Machine Toolpath Generation for Regions Bounded by Free Form Curves and Surfaces. Ph.D. Thesis, University of Utah, Computer Science Department, June 1989.

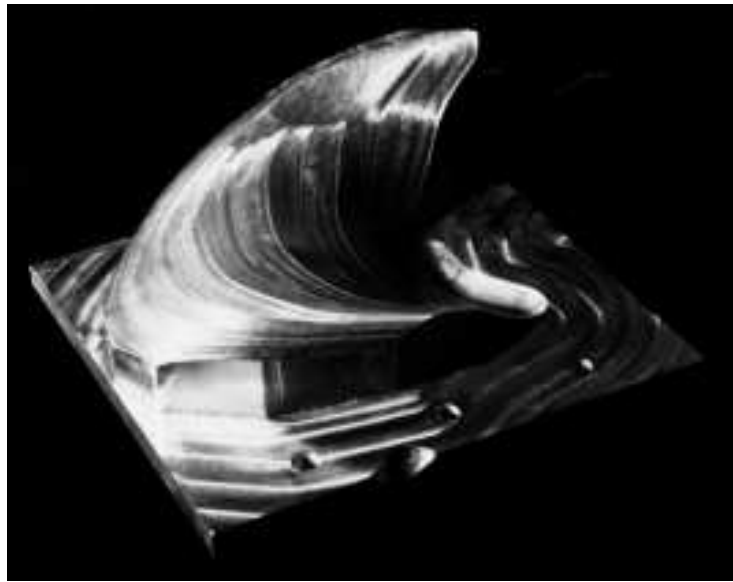
- [7] M. D. Carmo. *Differential Geometry of Curves and Surfaces*. Prentice-Hall 1976.
- [8] E. Cohen, T. Lyche, and L. Schumaker. Degree Raising for Splines. *Journal of Approximation Theory*, Vol 46, Feb. 1986.
- [9] E. Cohen, T. Lyche, and L. Schumaker. Algorithms for Degree Raising for Splines. *ACM Transactions on Graphics*, Vol 4, No 3, pp.171-181, July 1986.
- [10] E. Cohen, T. Lyche, and R. Riesenfeld. Discrete B-splines and subdivision Techniques in Computer-Aided Geometric Design and Computer Graphics. *Computer Graphics and Image Processing*, 14, 87-111 (1980).
- [11] G. Elber and E. Cohen. Error Bounded Variable Distance Offset Operator for Free Form Curves and Surfaces. *International Journal of Computational Geometry and Applications*, Vol. 1., No. 1, pp 67-78, March 1991.
- [12] G. Elber and E. Cohen. Tool Path Generation for Freeform Surface Models. Second ACM/IEEE Symposium on Solid Modeling and Applications, Montreal Canada, May 1993. Also to appear in CAD.
- [13] G. Elber. Accessibility in 5-Axis Milling Environment. To Appear in CAD.
- [14] G. Elber and E. Cohen. Exact Computation of Gauss Maps and Visibility Sets for Freeform Surfaces. In preparation.
- [15] G. Elber. Model Fabrication using Surface Layout Projection. To appear in CAD.
- [16] G. Elber. Freeform Surface Region Optimization for Three- and Five-Axis Milling. Submitted for publication.
- [17] R. Ferstenberg, K. K. Wang and J. Muckstadt. Automatic Generation of Optimized 3-Axes NC Programs Using Boundary Files. *IEEE 1986 International Conference on Robotics and Auto*, pp 325-332.
- [18] R. B. Jerard, J. M. Angleton and R. L. Drysdale. Sculptured Surface Tool path Generation with Global Interference Checking. *Design Productivity Conference*, Feb. 6-8, 1991, Honolulu, Hawaii.
- [19] G. C. Loney and T. M. Ozsoy. NC Machining of Free Form Surfaces. *Computer Aided Design*, vol. 19, no. 2, pp 85-90, March 1987.
- [20] T. Saito and T. Takahashi. NC machining with G-buffer method. *Computer Graphics*, Vol. 25, no. 4, pp 207-216, July 1991 (Siggraph 91).

- [21] S. W. Thomas. Scanline Rendering for 3-Axis NC Toolpath Generation, Simulation and Verification. Dept. of Electrical Engineering and Computer Science, University of Michigan, Ann Arbor, MI 48109-2122, Technical Report CSE-TR-43-90, January 1990.
- [22] D. Zhang and A. Bowyer. CSG Set-Theoretical Solid Modelling and NC Machining of Blend Surfaces. The Second Computation Geometry Conference, ACM 1986.



**Plate 1**

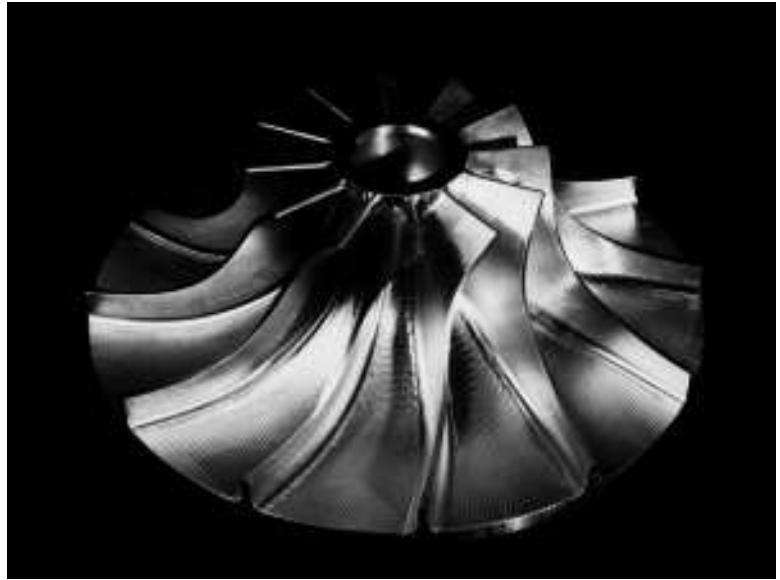
*Final machined examples of the model airplane's propeller. Shown are the original wooden propeller (top) along with two propellers machined from aluminum, without (middle) and with (bottom) their fixtures.*



**Plate 2**

*Final machined examples of the marine propeller's blade. Only top side of the blade was machined due to the difficulties in fixturing the blade.*



**Plate 3**

*Final machined examples of the centrifugal compressor. The air flow tunnels in this part were machined using the piecewise ruled surface side milling technique and with a conical tool.*